Novel Rechargeable Lithium-ion Battery Based on a Cathode of Cobalt Octacyanomolybdate

Journal:	*Journal of The Electrochemical Society*
Manuscript ID	JES-105177.R1
Manuscript Type:	Research Paper
Date Submitted by the Author:	n/a
Complete List of Authors:	Rojas, Victor; Pontificia Universidad Catolica de Valparaiso, Instituto de Quimica Cáceres, Gustavo; Pontificia Universidad Catolica de Valparaiso, Instituto de Quimica López, Silvana; Pontificia Universidad Catolica de Valparaiso, Instituto de Quimica Henríquez, Rodrigo; Pontificia Universidad Católica de Valparaíso, Instituto de Química Grez, Paula; Pontificia Universidad Católica de Valparaíso, Instituto de Química Navarrete, Emilio; Pontificia Universidad Catolica de Valparaiso, Instituto de Quimica Herrera, Francisco; Universidad de Santiago de Chile, Departamento de Química de los Materiales Caballero, Alvaro; Universidad de Córdoba Gómez-Cámer, Juan Luis; Universidad de Córdoba, Departamento de Química Inorgánica e Ingeniería Química Munoz, Eduardo; P. Catholic University, Institute of Chemistry
Keywords:	novel cathode cobalt octacyanomolybdate, experimental design, lithium-battery

Novel Rechargeable Lithium-ion Battery Based on a Cathode of Potassium-Cobalt(II) Octacyanomolybdate.

Víctor Rojas[1], Gustavo Cáceres[1], Silvana López[1], Rodrigo Henríquez[1], Paula Grez[1], Emilio Navarrete[2], Francisco Herrera[3], Álvaro Caballero[4], Juan Luis Gómez-Cámer[4,a], Eduardo Muñoz[1*].

[1]*Pontificia Universidad Católica de Valparaíso, Instituto de Química, Facultad de Ciencias, Av. Universidad 330, Valparaíso, Chile.*

[2]*Universidad de La Frontera, Departamento de Ciencias Químicas y Recursos Naturales, Facultad de Ingeniería y Ciencias. Av Francisco Salazar 01145, Temuco, Chile.*

[3]*Universidad de Santiago de Chile, Departamento de Química de los Materiales, Facultad de Química y Biología, Av. Libertador Bernardo O'higgins 3363 Estación Central, Santiago, Chile.*

[4]*Universidad de Córdoba, Departamento Química Inorgánica, Instituto Universitario de Investigación en Química Fina y Nanoquímica, Campus de Rabanales, Universidad de Córdoba, España.*

[1*] Corresponding author, eduardo.munoz.c@pucv.cl

[a] ISE member.

Abstract

In this work, the influence of the synthesis parameters (concentration, temperature, and reaction time) on the electrochemical performance of potassium-cobalt(II) octacyanomolybdate (KCoOCM) as a cathode material for its application in lithium-ion batteries was studied. The compound was synthesized hydrothermally using a chemometric approach and characterized by different techniques. The KCoOCM showed a change in its morphology from prismatic structures to nanorods according to the synthesis conditions. Additionally, there was an influence on the specific capacity as a function of the synthesis parameters, i. e., precursor's concentrations, temperature, and reaction time. The capacity values reached by the material was 50 mAh g^{-1}, which is close to the theoretical value of the KCoOCM (60 mAh g^{-1}). The statistical method employed would allow finding a condition where it is possible to maximize the capacity value of the material, which has been scarcely studied in this area. Finally, the performance of a lithium-ion battery based on a cathode of KCoOCM is reported for the first time in literature.

Keywords: novel cathode potassium-cobalt octacyanomolybdate, experimental design, lithium-battery

Introduction.

The development of new rechargeable batteries requires ongoing studies about cathode and anode compounds capable of reversibly inserting ions. Several reports have suggested hexacyanoferrates (HCF) family, promising low-cost and easy-to-prepare candidates for use in rechargeable batteries. Its open cubic structure, electrochemical reversibility, and stable interstitial sites allow the electrochemical insertion of ions from the electrolytic medium [1, 2]. It has been reported that the presence of interstitial water and the low crystallinity of these cathode compounds restrict its opportunity for practical applications [3]. Recently (January 2021) Qin and Col. have reported the synthesis of highly crystalline Prussian blue (H-PB) through a chemical inhibition strategy as an optimization tool in its use as a cathode in sodium-ion batteries (NaB), exhibiting a capacity of 78 mAh g^{-1} at 100°C and life-time of 2000 cycles at 10°C, with a retention of 62% [4]. Besides, Chen and Col. considered the modulation of PB and PB analogs properties from the synthesis parameters. They suggest adequate to explore the use of V, Cr, Mo, and W as active redox centers since these high valence metals can create lattice distortion capable of influencing these compounds' rate and energy storage capacity [5]. In this way, octacyanometallates (OCM) present certain similarities to HCF, and the most representative exponents are octacyanotungstates ($[W(CN)_8]^{3-/4-}$) and octacyanomolybdates ($[Mo(CN)_8]^{3-/4-}$) [6]. They present a higher coordination index than HCF, with frameworks in various dimensions (1D, 2D, 3D), two crystalline structures (square and dodecahedral antiprism) different from HCF, and two stable redox states ($[M^{V}(CN)_8]^{3-}/[M^{IV}(CN)_8]^{4-}$), allowing the electrochemical insertion of ions within their cavities [7, 8]. These compounds have been little addressed in the literature for their use in energy storage systems. It has been reported one study with $Tb(H_2O)_5[W(CN)_8]$

for Li-ion insertion [8]. This system displays quasi-reversible electrochemical signals, with a cell operating voltage of 3.3 V and gravimetric capacities of 30 mAh g^{-1}. The use of $[Mn(H_2O)][Mn(HCOO)_{2/3}(H_2O)_{2/3}]_{3/4}[Mo(CN)_8]\cdot H_2O$ system allowed the insertion of Li^+ and Na^+ ions with quasi-reversible redox processes of $[Mo^{V}(CN)_8]^{3-}/[Mo^{IV}(CN)_8]^{4-}$ [9].

In the present work, the electrochemical insertion of Li-ions in potassium-cobalt(II) octacyanomolybdate (KCoOCM) present in a secondary battery cathode was studied. This study was accompanied by an experimental design identifying and correlating the significance of the synthesis parameters as a function of the assembled batteries' performance. This work contributes to the knowledge of the synthesis, characterization, and use of KCoOCM as a cathode in a lithium battery, which has been scarcely addressed in the literature.

Experimental Section

The optimization of the synthesis variables of potassium-cobalt(II) octacyanomolybdate (KCoOCM) was carried out using a chemometric approach. A two-level factorial design was used to obtain the total number of synthesis conditions and, therefore, to evaluate its statistical significance. The variables considered in this study were the concentration of the precursors, temperature, and reaction time. The values assigned for each factor are presented in the following table:

Table I: Variables (experimental and coded) used in the experimental design to synthesize potassium-cobalt(II) octacyanomolybdate.

Synthesis of KCoOCM			
Factor	−1	0	+1
Co^{+2}: $Mo(CN)_8^{4-}$:KCl (M)	[0.1:0.1:1]	[0.2:0.2:1]	[0.4:0.4:1]
T (°C)	30	60	90
t (h)	2	5	8

Synthesis of potassium octacyanomolybdate, $K_4Mo(CN)_8$.

50 g of pure molybdenum oxide (IV) was dissolved in a 40% w/v potassium hydroxide solution. 250 mL of HCl was added slowly and under constant stirring to the solution. The resulting mixture was heated in a water bath until complete dissolution. A concentrated potassium thiocyanate solution was then prepared by dissolving 150 g of the salt in 150 mL of water. This solution was added slowly and with constant stirring to the hot solution of

molybdic acid generated before. This reaction has a deep red coloration, and was diluted with 300 mL of water and heated in a water bath for 2 hours with constant stirring. The solution was filtered, and 75 mL of pyridine was added slowly to the reaction product under constant stirring until a yellow solid appeared. The beaker was placed in an ice bath until a very viscous red oil appeared at the beaker's bottom. The product was allowed to decant and was washed two times with deionized water. The liquid oil was added to a solution containing 200 g of potassium cyanide in 300 mL of water. The yellow-brown solution obtained was heated in a water bath for 30 min. The black by-product was separated from the solution by decantation. The filtrate was heated to reduce its volume by 50%. Once concentrated, it was cooled in an ice-water bath, obtaining dark amber crystals, which were recovered by vacuum filtration. The crude product contains a considerable amount of black contaminants. It was dissolved in the minimum amount of boiling water for its purification, activated carbon was added, and then filtered. Ethanol was added in small amounts to the obtained solution until a golden yellow crystalline solid precipitated. The crystals were separated by vacuum filtration and washed sequentially with ethanol, ether, and dried in an oven at 80ºC.

Synthesis and purification of potassium-cobalt(II) octacyanomolybdate (KCoOCM).

The KCoOCM was in a closed system by using $K_4[Mo(CN)_8]$ and $CoCl_2$, and KCl as potassium charge to the compound. 20 mL of each solution was mixed in a 100 mL beaker with constant stirring for 10 minutes. At the end of this time, the mixture was transferred to a Teflon cell in a stainless-steel autoclave reactor where the temperature and time program corresponding to the experimental design was applied. After the reaction, the reactor was cooled to room temperature, obtaining a colloidal solution centrifuged at 4500 rpm to separate the solid from the supernatant. The product, potassium-cobalt(II)

octacyanomolybdate, was washed three times with deionized water and allowed to dry in an oven at 60 ° C. The precursor's concentrations are detailed in Table I.

KCoOCM cathode preparation.

The compounds obtained were mixed with a binder and a conductive additive. The purpose of including a binder was to strengthen its mechanical properties, keep the material particles together, and prevent spraying. The conductive additive was used to improve the conductivity of the mixture. Polyvinylidene fluoride (PVDF) and super P carbon were used as a binder and a conductive additive, respectively. The electrode was prepared by mixing the KCoOCM powders with super P carbon and PVDF in proportions of 80:10:10, respectively, in N-Methyl-2-Pyrrolidone (NMP) for 30 minutes at 4000 rpm using an Ultra-turrax disperser (Ika). The resulting suspension was deposited on a carbon stream collector (Gas Diffusion Layer, GDL) through the Doctor Blade technique, in which the active material is spread over the GDL with drag blades. The deposited material was dried at 50°C in an oven to evaporate all the solvent used. Finally, the KCoOCM electrodes were cut in discs with a diameter of 13 mm and weighed. They were vacuum dried in a glass oven (Buchi) at a temperature of 100°C for 3 hours.

Lithium-ion battery assembly.

The coin-type cells used were CR2032 model (20 mm in diameter and 3.2 mm in thickness). They consist of a pair of steel housings that act as current collectors that fit into an electrode holder connected to the measurement equipment. These two housings are electrically insulated by a plastic ring that joins them and allows their hermetic closure. For better conduction, a steel disc is used as an additional collector and a steel spring that fixes the internal components' position. The assembly is closed by adjusting with a hydraulic press

that makes the plastic ring expand, ensuring the cell's hermeticity. The cells were assembled in an MBraun 150 glove box under a controlled argon atmosphere.

The electrochemical behavior of the synthesized compounds was evaluated in a half-cell format. This configuration consists of facing the cathodic material against a metallic lithium disk with a diameter of 13 mm; The two electrodes were separated by a 16 mm diameter glass fiber Whatman filter impregnated with 1 M $LiPF_6$ electrolyte in a mixture of ethylene carbonate: diethyl carbonate (EC:DEC 50:50 by volume).

Cyclic voltammetry (CV) measurements were performed using a potenciostat/galvanostat (Autolab, PGSTAT204) in the potential range of 3.0 – 4.3 V vs Li^+/Li. Galvanostatic charge/discharge cycling tests of the cells were performed in a voltage of 3.0 – 4.3 V vs Li^+/Li in a battery tester Arbin BT2143. The program employed started in discharge mode from open-circuit voltage (3.2 V vs. Li^+/Li) until 3.0 V, and later was charged until 4.3 V.

Results and discussions.

For constructing the matrix of experiments, a two-level factorial design and three synthesis variables were considered [10, 11, 12]. The total number of experiments to be carried out was determined by $N = 2^k$. Where N corresponds to the total number of experiments and k to the number of experimental variables. Table II shows the matrix, which corresponds to 12 experiences, including four central points.

Table II: Matrix of experiments corresponding to the factorial design.

Exp.	1	2	3	4	5	6	7	8	9	10	11	12
Concentration	–1	+1	–1	+1	–1	+1	–1	+1	0	0	0	0
Temperature	–1	–1	+1	+1	–1	–1	+1	+1	0	0	0	0
Reaction time	–1	–1	–1	–1	+1	+1	+1	+1	0	0	0	0

Hydrothermal synthesis has been widely studied because highly crystalline structures are obtained, and the organization and growth of the structures are controlled. It is expected the obtention of structures of different sizes and morphologies. The reaction can be summarized by:

$$K_4Mo(CN)_{8(aq)} + CoCl_2 \times 2H_2O_{(aq)} \rightarrow K_2Co[Mo(CN)_8] \times nH_2O_{(s)} + 2KCl_{(aq)} + 2H_2O_{(l)}$$

X-ray diffraction (XRD).

Potassium-cobalt(II) octacyanomolybdate, KCoOCM, has been a compound little studied in the literature for application as a cathode in batteries. Because of this, there are no powder XRD standards to compare. Figure 1 shows the results for the 12 KCoOCM samples, where it is possible to appreciate the increase in the compounds' crystallinity in experiments 1, 3, 5,

and 7, where the synthesis temperature is the lowest in the experimental design. This condition causes a slower growth of the crystals, thus improving their crystallinity.

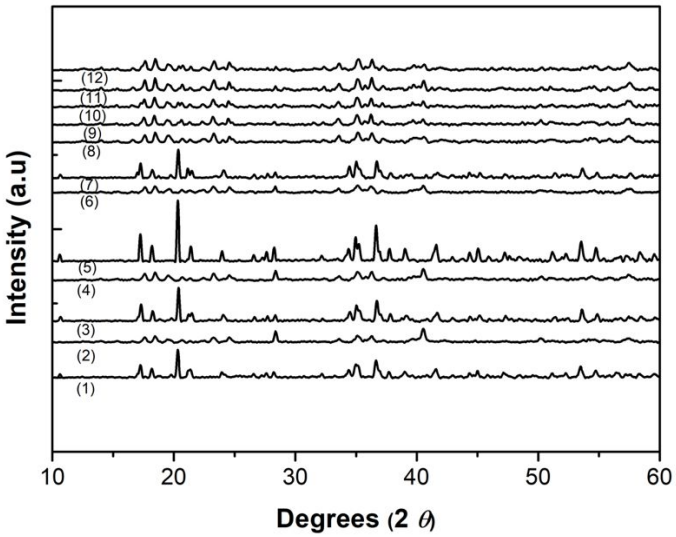

Figure 1: XRD patterns of the as-synthesized $K_2Co[Mo(CN)_6]$ samples.

Although it cannot be compared with a diffraction pattern, similar results have been reported for the synthesis of $Cu_2[Mo(CN)_8]$, where the most intense signal is close to 20º [13]. Cobalt octacyanomolybdates' fundamental structure is usually represented simultaneously under three spatial configurations: square antiprism, dodecahedron, or bicapped trigonal prism. Molybdenum is located at the center of these structures, carbon atoms are located in each vertex, and nitrogen atoms are attached to the cobalt atom [14].

Characterization by FESEM.

The co-precipitation of KCoOCM in the presence of excess Co^{2+} proceeds more slowly, allowing for ordered growth of highly crystalline, polydisperse nanoparticles. Field emission scanning electron microscopy (FESEM) was used to study the morphology of the KCoOCM.

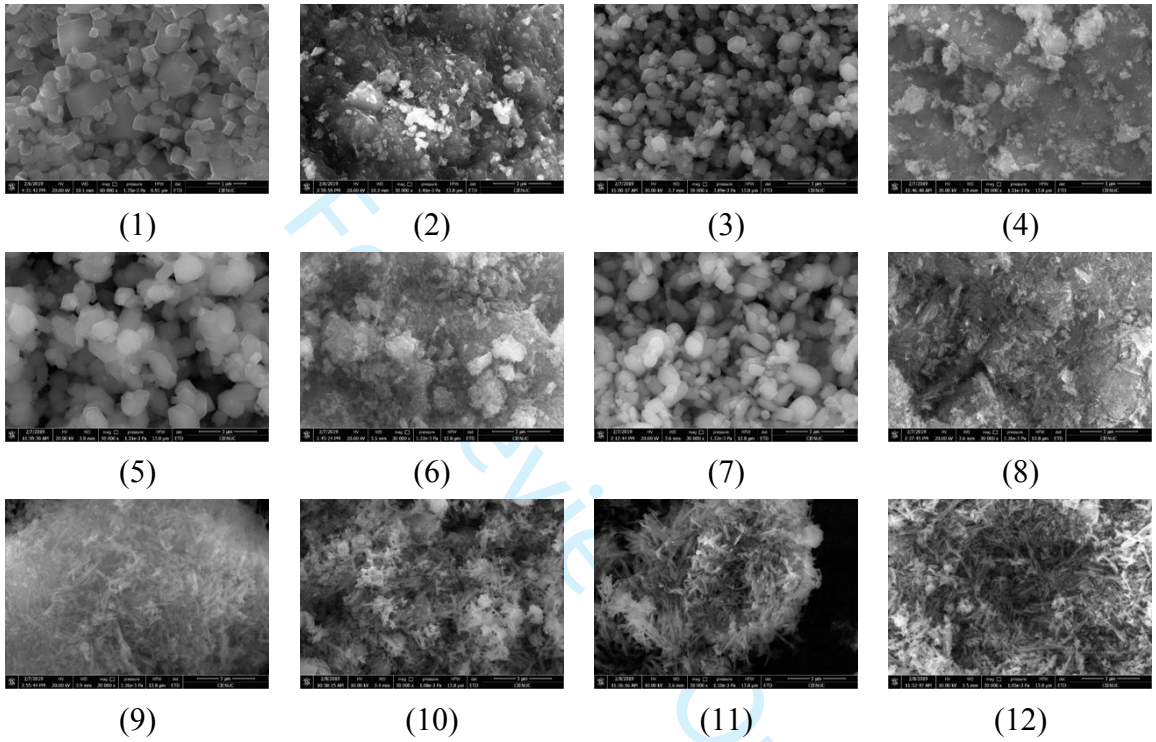

Figure 2: FESEM images for twelve samples of KCoOCM particles.

In addition to the images obtained, atomic absorption analysis shows that in the highest percentage of the synthesized samples, the stoichiometric relationship between molybdenum and cobalt is close to 0.7 (cf. Table 1S supplementary material), which indicates that the compound would have a molecular formula of $K_2Co[Mo(CN)_8]_{0.7}$, due to the presence of vacancies in its structure. As was demonstrated in the XRD study, the samples obtained from experiments 1, 3, 5, and 7 have more defined structures than the structures found in the other

samples. This confirms the obtention of more defined patterns due to the higher crystallinity of the compounds. With increasing temperature, Experiments 2, 4, and 6 are amorphous. However, by increasing the three synthesis variables in experiments 8, 9, and the four central points, the morphology changes drastically, obtaining CoOCM nanorods whose measure is between 30 and 50 nm width. The difference between experiments 8, 9, and the central points is that the higher synthesis conditions cause the growth of less well-defined nanorods and a more significant disorder than the central points, attributing this to the higher concentration of precursors.

Electrochemical studies.

The study was carried out using cyclic voltammetry to evaluate the stability of the material, reversibility, and redox processes' potentials. Figure 3 shows a lithium half-cell's potentiodynamic profile with KCoOCM as cathode at a scan rate of 0.1 mV s^{-1} in a potential window of 3.0 V - 4.3 V vs. Li^{+}/Li. A cathodic and an anodic current peak can be seen at potentials of 3.8 V and 3.95 V, respectively, which correspond to the redox processes of molybdenum (Mo^{4+}/Mo^{5+}) carbon-coordinated. This type of Prussian Blue analogue has only one active center because cobalt nitrogen-coordinated has such a low solubility product that a reduction of this metal ion shifts to an inaccessible value [15]. The voltammogram corresponds to the sample obtained from the first point of the synthesis.

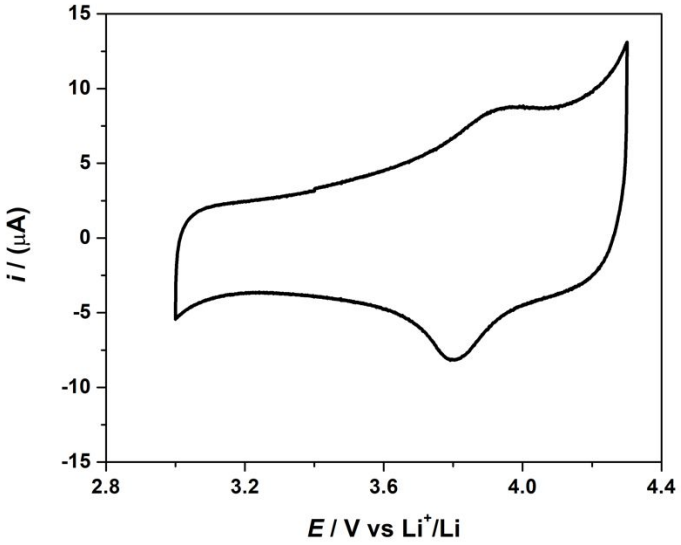

Figure 3: CV of a lithium half-cell with a cathode based on KCoOCM. Scan rate 0.1 mV s^{-1} and potential range of 3.0 – 4.3 V vs Li^+/Li.

The specific capacity for ten cycles for the twelve samples was determined by applying a current rate of 1 C (60.8 mAh g^{-1}). In Figure 4, the best results correspond to sample number 7 with a capacity close to 45 mAh g^{-1}. The synthesis with the lowest performance was sample number 1, with a value close to 8 mAh g^{-1}. The samples obtained from experiments 2, 4, and 6 did not show electrochemical activity attributed to their amorphous structures (low crystallinity), demonstrating the importance of this parameter in the batteries' performance. The samples obtained from the central points, show the same behavior with values close to 20 mAh g^{-1}. The graph shows the results from cycles 1 to 10.

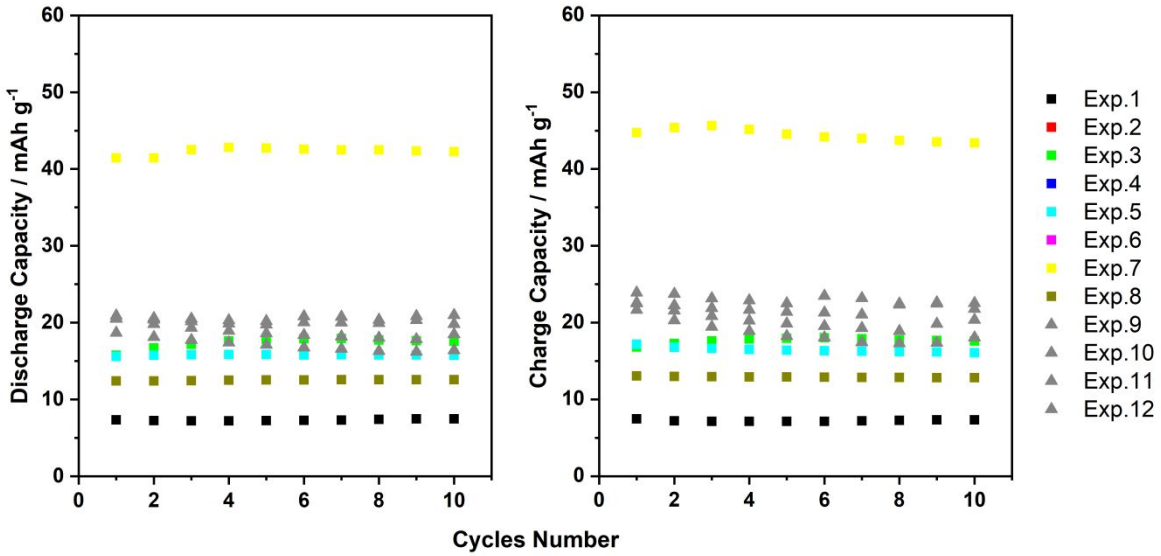

Figure 4: Specific Capacity as function of cycle number for twelve samples. C-rate 1C.

Table IV: Average of the Specific Capacities for twelve samples.

Sample	1	2	3	4	5	6	7	8	9	10	11	12
Disch. cap./mAhg^{-1}	7.3	0	17.4	0	15.8	0	42.3	12.5	18.8	20.4	17.1	20.3
Charge cap./mAhg^{-1}	7.2	0	17.6	0	16.5	0	44.4	12.9	20.3	22.0	18.7	23.0

As seen from FESEM images, there exists a dependence between morphology and synthesis conditions. The sample obtained from experiment 7, which presented the higher capacity, was synthesized at low precursor concentrations, high temperature, and high reaction time, obtaining structures with a higher crystallinity and smaller particles. The sample obtained from experiment 8 (highest synthesis conditions) shows a structure change from hexagonal to nanorod-type.

Statistical analysis for specific charge responses was carried out [16]. In Figure 5, a Pareto diagram obtained through the StatGraph program is shown.

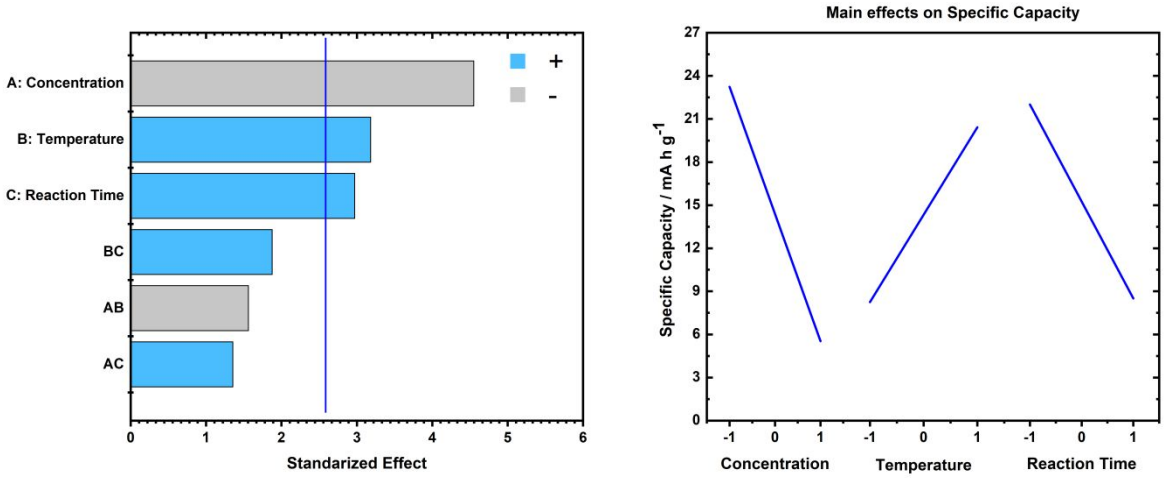

Figura 5: (a) Standarized Pareto diagram for discharge specific capacity. (b) Principal effects graph for discharge specific capacity.

The Durbin-Watson statistic has a value of 2.57. In this design, all variables are significant, i. e., precursors' concentration, temperature, and reaction time. The dependence of these variables indicates an increase in the precursors' concentration decreases the sample's discharge capacity, while an increase in temperature and reaction time produces an increase in the sample's discharge capacity. This dependence is shown in Figure 5b.

The decrease in the battery capacity due to the increase in the precursor's concentration has particular relevance. There is a difference of 20 mAh g^{-1} between the extreme values. The influence of this variable can be associated with more crystalline structures and morphology with defined geometry at low concentrations. Meanwhile, there is a significant presence in solution at higher precursor concentrations, producing many agglomerates and obtaining

more amorphous structures. An increase in temperature causes a more significant interaction between the precursor's molecules and an increase in the closed system's internal pressure. Finally, longer reaction times have a positive effect on the capacity. This is attributed to the formation of a more significant number of particles as a function of time. By combining this variable with an increase in temperature, particles with a rod-like morphology are generated, totally different from the initial ones, showing a dependence in the morphology. Variance analysis for the statistical model allows to contrast results. The three individual significant variables have a P-value lower than 0.05, comparing their mean square against an estimate of the experimental error, which indicates that they are significantly different from zero with a 95% confidence level. According to the ANOVA table (cf. supplementary material), the experimental data follow linearity since the R-square presents a value close to 91%. The preceding is very important since, through the data shown, it will be possible to maximize the charge capacity of a KCoOCM cathode obtained under determined precursor concentration, temperature, and reaction time. Additionally, the Table shows the specific capacity obtained experimentally and from the application of the statistical model, which is given according to the following equation:

$$Y = A_0 + A_1X_1 + A_2X_2 + A_3X_3 + A_{12}X_1X_2 + A_{13}X_1X_3 + A_{23}X_2X_3 + A_{123}X_1X_2X_3$$

Where, Y corresponds discharge specific capacity, A_0 a constant, A_1, A_2, and A_3 correspond to the regresion coefficients, meanwhile X_1, X_2, and X_3 to the individual variables from the design. In Table V, the regresion coefficients are shown.

Table V: Regression coefficients for discharge specific capacity.

Coefficient	Constant	A: Prec. Conc.	B: Temp.	C: Reaction time	AB	AC	BC
Estimate	14.3	-8.79	6.14	5.74	-3.01	-2.61	3.61

Besides, a table with the observed and the adjusted values of the battery capacity was constructed:

Table VI: Discharge specific capacity values: observed and adjusted.

Sample	1	2	3	4	5	6	7	8	9	10	11	12
Obs. values	7.3	0.0	17.4	0.0	15.8	0.0	42.3	12.5	18.8	20.4	17.1	20.3
Adjust. values	9.2	2.9	20.3	1.9	18.7	1.9	44.2	15.4	14.3	14.3	14.3	14.3

According to Table VI, the central points' average is very close to the experimental values indicating the experiments' design's linearity. Therefore, no additional adjustments are necessary. The procedure is validated with the residuals' values that do not exceed the standard error of 5.46. (cf. Table 2S supplementary material)

Finally, it is possible to build the predictive model that accounts for the variation of the specific discharge capacity with the significant experimental variables:

$$\text{Spec. disch. cap.}\left(\text{mAh g}^{-1}\right) = 14.325 - 8.7875 \cdot [\text{P}] + 6.1375 \cdot \text{T}^{\circ} + 5.7375 \cdot \text{t}$$

where [P] is the precursor's concentration, T° is the temperature, and t is the reaction time. As they are not significant in the response, the interactions between the variables can be omitted from the equation.

After the statistical analysis, the electrochemical study focused on the sample obtained from experiment 7, which has the highest capacity value at a C-rate of 1C. The appropriate rate was determined for the study of cyclability and coulombic efficiency through the C-Rate technique, in which the capacity for different speeds during ten cycles was obtained. Figure 6a shows the variation in storage capacity from 50 mAh g^{-1} at C/20 to values close to 40 mAh g^{-1} at 1C. Once the C/20 rate was restored, the capacity recovers the values close to the initial ones, demonstrating the battery's cyclability and stability.

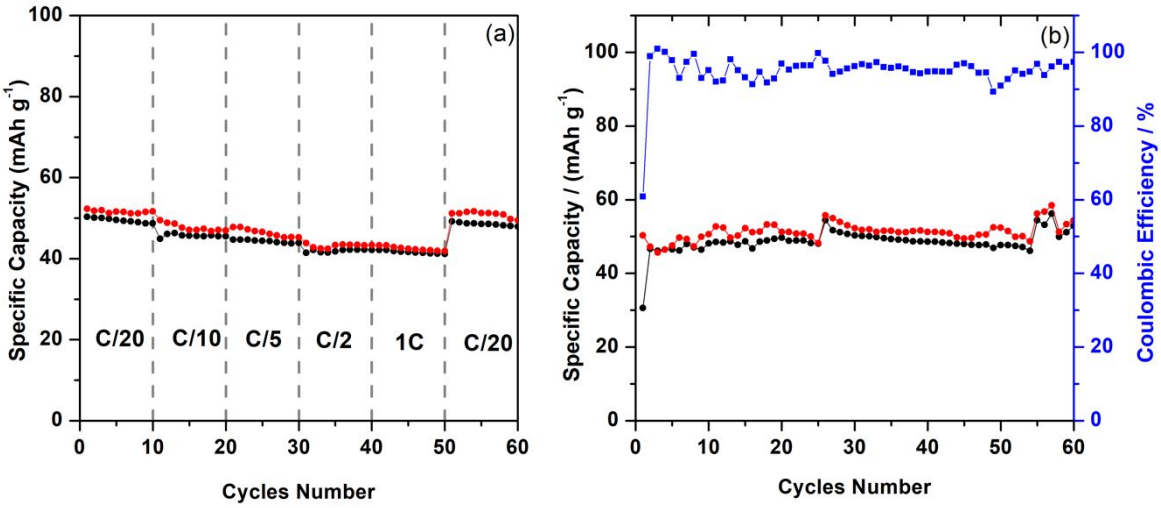

Figure 6: a) Specific capacity as function of cycle numbers for sample 7; b) specific capacity and the coulombic efficiency at C/20 for sample 7. The electrolyte used was $LiPF_6$ 1 M in EC:DEC 50:50.

The theoretical capacity for $K_2Co[Mo(CN)_8]$ is 60.8 mAh g^{-1} in its anhydrous form. Through the ATG analysis (cf. Fig. 1S suppl. material), it was possible to determine five more water molecules ($K_2Co[Mo(CN)_8]\times5H_2O$). Accordingly, it could be expected a decrease in capacity from 60.8 mAh g^{-1} to value ca. 50 mAh g^{-1}. In practice, the capacities of the Prussian

blue analogs are lower than the theoretical capacities due to the adsorbed and zeolitic water [17]. The presence of vacancies and coordinated water in the structure of these compounds, cause a variety of adverse effects that severely deteriorate the electrochemical performance of KCoOCM framework. First, the increase in the vacancies should introduce more water molecules into KCoOCM to coordinate with the dangling Li^+ ions, thus decreasing the available sites to host Li^+ ions and therefore leading to a loss of the usable Li-insertion capacity. Second, the zeolitic water molecules have a strong tendency to reside in or to compete with Li^+ ions to occupy the interstitial spaces, which may block the transport of Li^+ ion into the lattice, thereby lowering the capacity utilization of Prussian Blue analogues framework [18]. Despite the above, the results show an identical capacity to the theoretical one of the hydrated compound, and additionally, a high coulombic efficiency of 96%. This behavior demonstrates the good electrochemical reversibility of KCoOCM, charging and discharging for 12 hours for each process. Although there are few cycles, it is expected more than 100 cycles will be studied for this compound soon. Table VII shows a comparison between results obtained for different cathodes based on metal hexacyanometallates. The capacity obtained by the KCoOCMo synthesized in this work is within the values obtained for various types of Prussian blue analogs with a metal center, unlike the FeHCF and LiPB-PPy-PPs compounds have twice the capacity due to their two active metal centers that can undergo electrochemical insertion processes.

Table VII: Comparative results of compounds belonging to cyanometallates obtained from references.

Compound	Ref.	Working potential / V	Synthesis method	C-rate	Capacity / mAh/g
KCoOCM*	*	3.9	Hydrothermal	C/20	50
NiHCF	[19]	3.3	Co-precipitation	C/5	52
CuHCF	[20]	3.6	Co-precipitation	C/20	60
MnHCF	[21]	3.5	Sol-gel	83 C	40.1
FeHCF	[22]	3.1	Co-precipitation	3C	138
LiPB-PPy-PPs	[23]	3.5	Co-precipitation	3C	119

* Cathode material obtained in this work.

Conclusions

A chemometric approach for the synthesis of potassium-cobalt(II) octacyanomolybdate allowed the obtention of particles with clear dependence of its morphology with the synthesis conditions, obtaining prismatic structures for the lowest and nanorod-type structures for the highest conditions. The experimental design analysis showed a dependence of the battery's storage capacity with the morphology of the particles. The sample obtained under conditions: −1(lower concentration); +1(higher temperature); +1 (higher reaction time), showed the best capacity results due to reducing the diffusion length of lithium ions in a structure nanorod-type. The opposite case was the synthesis conditions that generated structures with low crystallinity, which did not show electrochemical activity. The experiment with the best results (Exp. 7) presented average capacity values of approximately 50 mAh g^{-1} during sixty

charge/discharge cycles. These results are very close to the theoretical capacity (60.1 mAh g^{-1}) of the material, being diminished by the influence of water absorbed or present structurally in the compound. The capacities obtained are well below commercial materials. However, the strategy used showed that the control of the synthesis variables allows finding a condition in which the material's performance is increased, which could be applied in other types of compounds. Finally, it was possible to evaluate the performance of a lithium-ion battery based on a cathode of KCoOCM, which has not been addressed in the literature yet.

Acknowledgements

We acknowledge the financial support from FONDECYT, Chile, (grant no. 1240108), from VRIEA-PUCV (grant no. 039.438 NÚCLEO-PUCV and 125.737/21 DII-PUCV), from the Spanish *Ministerio de Economía y Competitividad* (Project MAT2017-87541-R) and from *Junta de Andalucía* (Group FQM-175) and from FONDEQUIP EQM150101. E. Navarrete thank for the financial support from postdoctoral project FONDECYT (N° 3200216). V. Rojas would like to acknowledge the kind support from his doctoral scholarship by ANID Nº 21160733. F. Herrera thanks DICYT-USACH for their financial support.

References.

[1] M.T. Xia, X.K. Zhang, T. T. Liu, Commercially available prussian blue get energetic in aqueous K-ion batteries, Chem. Eng. J. 394 (2020) 124923. https://doi.org/10.1016/j.cej.2020.124923.

[2] W. Wang, Y. Gang, Z. Hu, Reversible structural evolution of sodium-rich rhombohedral Prussian blue for sodium-ion batteries, Nat. Commun. 11 (2020) 980. https://doi.org/10.1038/s41467-020-14444-4.

[3] S. Zhao, Z. Guo, K. Yan, The rise of prussian blue analogs: challenges and opportunities for high-performance cathode materials in potassium-ion batteries, Small Struct. 2 (2021) 2000054. https://doi.org/10.1002/sstr.202000054

[4] M. Qin, W. Ren, R. Jiang, Highly crystallized prussian blue with enhanced kinetics for highly efficient sodium storage, ACS Appl. Mater. Interfaces. 13 (2021) 3999-4007. https://doi.org/10.1021/acsami.0c20067.

[5] J. Chen, L. Wei, A. Mahmood, Prussian blue, its analogues and their derived materials for electrochemical energy storage and conversión, Energy Storage Mater. 25 (2020) 607. https://doi.org/10.1016/j.ensm.2019.09.024

[6] B. Sieklucka, R. Podgainy, R. Korzeniak, Supramolecular networks based on octacyanometallates of Mo and W, C. R. Chimie. 5 (2002) 639-649. https://doi.org/10.1016/S1631-0748(02)01428-5

[7] J. L. Hoard, T. A. Hamor, M. D. Glick, Stereochemistry of discrete eight-coordination. V. Octacyanomolybdate(IV) ion, J. Am. Chem. Soc. 90 (1968) 3177-3178. https://doi.org/10.1021/ja01014a037.

[8] J. Long, D. Asakura, M. Okubo, Electrochemical Li-Ion intercalation in octacyanotungstate-bridged coordination polymer with evidence of three magnetic regimes, Inorg. Chem. 55 (2016) 7637-7646. https://doi.org/10.1021/acs.inorgchem.6b01086

[9] M. Okubo, K. Kagesawa, Y. Mizuno, Reversible solid state redox of an octacyanometallate-bridged coordination polymer by electrochemical ion insertion/extraction, Inorg. Chem. 52 (2013) 3772-3779. https://doi.org/10.1021/ic302364d.

[10] Emilio Navarrete, Javier Román, Víctor Rojas, Rodrigo Henríquez, Ricardo Schrebler, Ricardo Córdova, Manuel Bravo, Eduardo Muñoz. Chemometric approach to study the influence of synthesis parameters on the size of CdTe quantum dots obtained from aqueous solutions Arabian Journal of Chemistry (2019) 12, 5103–5110. http://dx.doi.org/10.1016/j.arabjc.2016.10.011.

[11] Renzo Milesi L., Emilio Navarrete S., Javier Román S., Víctor Rojas C., Rodrigo Henríquez N., Ricardo Schrebler G., Ricardo Córdova, Eduardo C. Muñoz, A Chemometric Approach To The Influence Of The Synthesis Parameters On The Optical Response Of Gold Nanoparticles And Study Of Their Electrophoretic Deposition On Silicon. J. Chil. Chem. Soc., 61, (2016), 3228-3232.

[12] Sérgio Ferreira, Adriana Queiroz, Marcelo Fernandes, Hilda dos Santos. Application of factorial designs and Doehlert matrix in optimization of experimental variables associated with the preconcentration and determination of vanadium and copper in seawater by inductively coupled plasma optical emission spectrometry. Spectrochimica Acta Part B: Atomic Spectroscopy. 57 (12) (2002) 1939-1950. https://doi.org/10.1016/S0584-8547(02)00160-X.

[13] Shin-ichi Ohkoshi, Hiroko Tokoro, Toshiya Hozumi, Yue Zhang, Kazuhito Hashimoto, Corine Mathonière, Isabelle Bord, Guillaume Rombaut, Marc Verelst, Christophe Cartier dit Moulin, and Françoise Villain, Photoinduced Magnetization in Copper Octacyanomolybdate. J. Am. Chem. Soc. 2006, 128, 1, 270–277. https://doi.org/10.1021/ja0559092.

[14] P. Przychodze, T. Korzeniak, R. Podgajny, and B. Sieklucka. Supramolecular coordination networks based on octacyanometallates: From structure to function. Cordination Chem. Rev., vol. 250 (2006) 22 34–2260. https://doi.org/10.1016/j.ccr.2006.01.026.

[15] F. Scholz, H. Kahlert, Electrochemistry of Polycyanometallates, in: Encycl. Electrochem., 2006, 703–722, Wiley-VCH, Germany. https://doi.org/10.1002/9783527610426.bard070023.

[16] Massart, D.L., Vandeginste, B.G.M., Buydens, L.M.C., De Jong, S., Lewi, P.J., Smeyers-Verbeke, J., 1998. Handbook of Chemometrics and Qualimetrics: Part A. 1st ed. Elsevier, Amsterdam.

[17] C.D. Wessells, R.A. Huggins, Y. Cui, Copper hexacyanoferrate battery electrodes with long cycle life and high power. Nat. Commun. 2 (2011) 550–555. https://doi.org/10.1038/ncomms1563.

[18] A. Paolella, C. Faure, V. Timoshevskii, S. Marras, G. Bertoni, A. Guerfi, A. Vijh, M. Armand, K. Zaghib, A review on hexacyanoferrate-based materials for energy storage and smart windows: Challenges and perspectives, J. Mater. Chem. A. 5 (2017) 18919–18932. https://doi.org/10.1039/c7ta05121b.

[19]: M. Omarova, A. Koishybay, N. Yesibolati, A. Mentbayeva, I. Kurmanbayeva, Z. Bakenov, Nickel Hexacyanoferrate Nanoparticles as a Low Cost Cathode Material for

Lithium-Ion Batteries, Electrochim. Acta. 184 (2015) 58–63. https://doi.org/10.1016/j.electacta.2015.10.031.

[20]: V. Rojas, G. Cáceres, S. López, R. Henríquez, P. Grez, R. Schrebler, E. Navarrete, F. Herrera, A. Caballero, J. L. Gómez-Cámer, E. Muñoz, Rechargeable Lithium-Ion Battery Based on a Cathode of Copper Hexacyanoferrate, J. Electrochem. Soc., 168 (8) (2021) 080515. https://10.1149/1945-7111/ac1a53.

[21]: J. Song, L. Wang, Y. Lu, J. Liu, B. Guo, P. Xiao, J.J. Lee, X.Q. Yang, G. Henkelman, J.B. Goodenough, Removal of interstitial H2O in hexacyanometallates for a superior cathode of a sodium-ion battery, J. Am. Chem. Soc. 137 (2015) 2658–2664. https://doi.org/10.1021/ja512383b.

[22]: L. Shen, Z. Wang, L. Chen, Prussian Blues as a Cathode Material for Lithium Ion Batteries, Chem. - A Eur. J. 20 (2014) 12559–12562. https://doi.org/10.1002/chem.201403061.

[23]: D. Asakura, C.H. Li, Y. Mizuno, M. Okubo, H. Zhou, D.R. Talham, Bimetallic cyanide-bridged coordination polymers as lithium ion cathode materials: Core@Shell nanoparticles with enhanced cyclability, J. Am. Chem. Soc. 135 (2013) 2793–2799. https://doi.org/10.1021/ja312160v.